Science of the Total Environment 879 (2023) 163191

Contents lists available at ScienceDirect

Science of the Total Environment

journal homepage: www.elsevier.com/locate/scitotenv

Inter-regional environmental inequality under lasting pandemic exacerbated by residential response

Chunjin Li [a], Jintai Lin [a,*], Lulu Chen [a], Qi Cui [b], Yu Liu [c], Erin E. McDuffie [d,e], Mingxi Du [f], Hao Kong [a], Jingxu Wang [g,h]

[a] Laboratory for Climate and Ocean-Atmosphere Studies, Department of Atmospheric and Oceanic Sciences, School of Physics, Peking University, Beijing 100871, China
[b] School of Economics and Management, China University of Petroleum, Qingdao 266580, China
[c] College of Urban and Environmental Sciences, Peking University, Beijing 100871, China
[d] Department of Energy, Environmental and Chemical Engineering, Washington University in St. Louis, St. Louis, MO 63130, USA
[e] Department of Physics and Atmospheric Science, Dalhousie University, Halifax, NS B3H 4R2, Canada
[f] School of Public Policy and Administration, Xi'an Jiaotong University, Xi'an 710049, China
[g] Key Laboratory of Physical Oceanography, Ocean University of China, Qingdao 266100, China
[h] College of Oceanic and Atmospheric Sciences, Ocean University of China, Qingdao 266100, China

HIGHLIGHTS

- Combining changes in transportation, production and household behavior is key to assess pandemic's impact on air pollution.
- Pandemic-induced changes in activity levels and household energy choices could increase residential emissions.
- Global $PM_{2.5}$-related mortality under a persisting pandemic would be higher when including residential emission changes.
- The least affluent regions would suffer the highest fractional economic losses with no comparable mortality reduction.

GRAPHICAL ABSTRACT

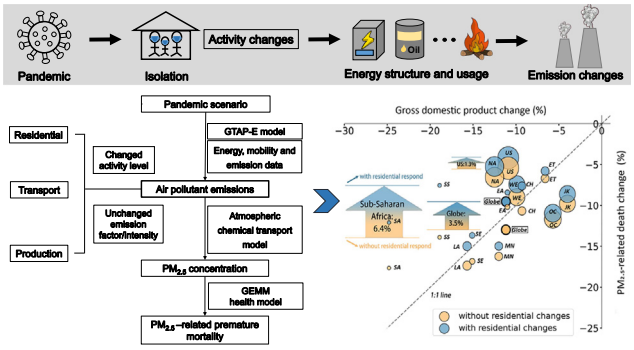

ARTICLE INFO

Editor: Jianmin Chen

Keywords:
Pandemic
Emission change
Air pollution related mortality
Residential response
Environmental inequality

ABSTRACT

Pandemics greatly affect transportation, economic and household activities and their associated air pollutant emissions. In less affluent regions, household energy use is often the dominant pollution source and is sensitive to the affluence change caused by a persisting pandemic. Air quality studies on COVID-19 have shown declines in pollution levels over industrialized regions as an immediate response to pandemic-caused lockdown and weakened economy. Yet few have considered the response of residential emissions to altered household affluence and energy choice supplemented by social distancing. Here we quantify the potential effects of long-term pandemics on ambient fine particulate matter pollution ($PM_{2.5}$) and resulting premature mortality worldwide, by comprehensively considering the changes in transportation, economic production and household energy use. We find that a persisting COVID-like pandemic would reduce the global gross domestic product by 10.9 % and premature mortality related to black carbon, primary organic aerosols and secondary inorganic aerosols by 9.5 %. The global mortality decline would reach 13.0 % had the response of residential emissions been excluded. Among the 13 aggregated regions worldwide, the least affluent regions exhibit the greatest fractional economic losses with no comparable magnitudes of mortality reduction. This is because their weakened affluence would cause switch to more polluting household energy types on top of longer stay-at-home time, largely offsetting the effect of reduced transportation and economic production. International financial, technological and vaccine aids could reduce such environmental inequality.

* Corresponding author.
E-mail address: linjt@pku.edu.cn (J. Lin).

http://dx.doi.org/10.1016/j.scitotenv.2023.163191
Received 13 January 2023; Received in revised form 21 March 2023; Accepted 27 March 2023
Available online 31 March 2023

1. Introduction

Human beings are at risk of newly or re-emerging infectious diseases due to climate change (Watts et al., 2018; Huber et al., 2020; Hueffer et al., 2020), and the occurrence of pandemics similar to COVID-19 is very likely in the future (Marani et al., 2021). The COVID-19 is a reminder that the global economy and environment are susceptible to sudden disruptions by pandemics. Coping with a pandemic means lockdown, economic downturn and household behavioral changes, which together affect emissions and ambient levels of air pollution. Indeed, since COVID-19 was declared as a pandemic (World Health Organization (WHO), 2020), many studies have shown evidence of reductions in emissions and pollution levels over industrialized regions (Lee et al., 2020; Mahato et al., 2020; Forster et al., 2020; Keller et al., 2021), and that changes in meteorological conditions and nonlinear chemistry may complicate the response of ambient pollution to the pandemic (Shen et al., 2021; Le et al., 2020; Hammer et al., 2021; Li et al., 2021; Huang et al., 2021; He et al., 2020). These studies have focused on the environmental effects of weakened transportation and economic activities as an immediate, short-term response within a few weeks or months of the start of the pandemic. Yet few have considered the changes in household affluence level and respective energy choice as a result of economic recession, especially in less affluent regions, when a pandemic persists for years.

Household fuel combustion for heating and cooking is the dominant source of air pollution over less industrialized regions (Tao et al., 2018; Lelieveld et al., 2015; Yun et al., 2020; Chen et al., 2018; Mbandi, 2020). Thus accounting for the changes in household energy use is important to reveal the full picture of the environmental impacts of a pandemic. First, lockdown means people stay at home for a longer period and require more fuels for heating and cooking (Kikstra et al., 2021; Elavarasan et al., 2020; Hook et al., 2020; Google, 2020), which tend to enhance residential emissions. Furthermore, when a pandemic lasts and the economy remains weakened, household income and financial capability will be cut substantially. Especially for less affluent regions, lowered affluence means undermined affordability to cleaner energy sources (electricity and gas) and forced switch to cheaper but more polluting fuels (biomass and coal). A change in household fuel structure is much easier than that for factories in terms of time and cost. For example, many stoves in the rural households can burn different fuels; and many rural households in China possess both gas- and coal-fired burners, suited for a swift switch (Tao et al., 2018; Chen et al., 2018). A field study of a Chinese village has shown increased residential coal consumption and resulting $PM_{2.5}$ pollution during the COVID-19 lockdown period (Li et al., 2021). However, a quantitative global analysis of the combined environmental effects of changes in economic activity and household behavior caused by lasting pandemics remains lacking.

The enduring pandemics' environmental impacts and corresponding health consequences might exacerbate environmental inequality across various regions. Environmental inequality has gained increasing attention from both researchers and policymakers in recent years. Existing literature on air pollution has highlighted a disproportionate burden of environmental pollution borne by minorities and low-income groups, which adversely affects their health (Zhang et al., 2018; Szasz and Meuser, 1997; Williams and Collins, 1995; Mackenbach et al., 1997; Lake, 1996). This situation may be worsened under a lasting pandemic because these residents in less affluent regions tend to use more polluting but cheaper energy as their incomes decrease. Thus, a quantitative analysis of inter-regional environmental equality under lasting pandemics is necessary.

Here we assess the potential effects of a persisting pandemic on ambient $PM_{2.5}$ pollution and associated premature mortality worldwide, by considering the emission changes associated with transportation, economic production and residential energy use. Briefly, we use an economic model (Burniaux and Truong, 2002) to simulate the economic changes in response to a persisting pandemic. We estimate the affluence-driven changes in household energy consumption by using historical energy data (Boden et al., 2017; Fernandes et al., 2007; British Petroleum Company, 2019; International Energy Agency (IEA), 2016), and consider the lockdown-induced variations in household activity and transportation mobility based on recent real-world statistics (Shen et al., 2021; Google, 2020; Apple, 2020). These data are combined with emission inventory data (McDuffie et al., 2020) to estimate the pandemic's effect on pollutant emissions, which are subsequently translated to ambient $PM_{2.5}$ concentrations using chemical transport model simulations (Chen et al., 2021; Lin et al., 2019; GEOS-Chem v11-01, 2017). Finally, we employ a health model (Burnett et al., 2018) to calculate premature mortality due to long-term exposure to ambient $PM_{2.5}$ (Chen et al., 2021; Lin et al., 2019). Our findings demonstrate that the residential response to a persistent pandemic leads to a significant escalation of inter-regional environmental inequality.

2. Materials and method

2.1. Framework

The framework of our methodology and the detailed emission calculation process are depicted in Fig. 1. To calculate emission changes under a persisting pandemic, we apply different types of perturbations to individual sectors based on their unique characteristics. For this purpose, we categorize the sectors into four main groups, including transportation (private and commercial), residential (resulting from household fuel combustion and electricity usage), agriculture, and industry (which includes power generation to support industrial production) (Supplementary Table 1).

As shown in Fig. 1, we use the Global Trade Analysis Project – Energy (GTAP-E) model (Burniaux and Truong, 2002) to simulate the effect of a persisting pandemic on the economy and fuel use in GDP-producing sectors. For residential energy, we use the historical data (Boden et al., 2017; Fernandes et al., 2007; British Petroleum Company, 2019; International Energy Agency (IEA), 2016) to construct statistical relationships between energy use and affluence for each region, and apply these relationships to the pandemic scenario. We also account for enhanced residential activity during lockdown due to lengthened stay at home. For transportation, we consider the effect of lockdown on mobility change as well as the impact of economic production changes on commercial transportation. We apply the emission factor/intensity data based on the IEA energy data (International Energy Agency (IEA), 2016), GTAP economic database (GTAP v10a Data Base, 2019) and $CEDS_{GBD\text{-}MAPS}$ emission inventory (McDuffie et al., 2020) in the pandemic scenario to obtain respective emissions for each region, pollutant type and sector. We employ the GEOS-Chem chemical transport model-derived chemical efficiency metrics (Chen et al., 2021; Lin et al., 2019; GEOS-Chem v11-01, 2017) to convert pollutant emissions to ambient concentrations for individual $PM_{2.5}$ compositions. Finally, we use the Global Exposure Mortality Model (GEMM) (Burnett et al., 2018) model to estimate the effect of $PM_{2.5}$ pollution changes on premature mortality.

We focus on a lasting pandemic similar to COVID-19 in terms of severity and socioeconomic responses (but not in terms of duration, see next paragraphs). In this way, we take advantage of the COVID-19 data to constrain model calculations, including mobility data from Google (Google, 2020), Apple (Apple, 2020) and Gaode Map (Gaode, 2020), socioeconomic statistics from CEIC (CEIC dataset, 2022), the International Labor Organization (ILO) (International Labor Organization (ILO), 2021) and the National Bureau of Statistics of China (NBSC) (National Bureau of Statistics of China (NBSC), 2021), and near-surface $PM_{2.5}$ concentration data from a satellite-based dataset (Hammer et al., 2021; Van Donkelaar et al., 2016) and ground stations (The World Air Quality Index Project (WAQI), 2022). We consider the changes in emissions of black carbon (BC), primary organic aerosols (POA) and those gases leading to secondary inorganic aerosols (SIOA), including sulfur dioxide (SO_2), nitrogen oxides (NOx) and ammonia (NH_3). Following our previous studies (Lin et al., 2019; Du et al., 2020), countries are aggregated into 31 regions for economic simulations and emission calculations, and further into 13 regions for subsequent calculations of ambient pollution levels and associated mortality; see regional definitions in Supplementary Fig. 1.

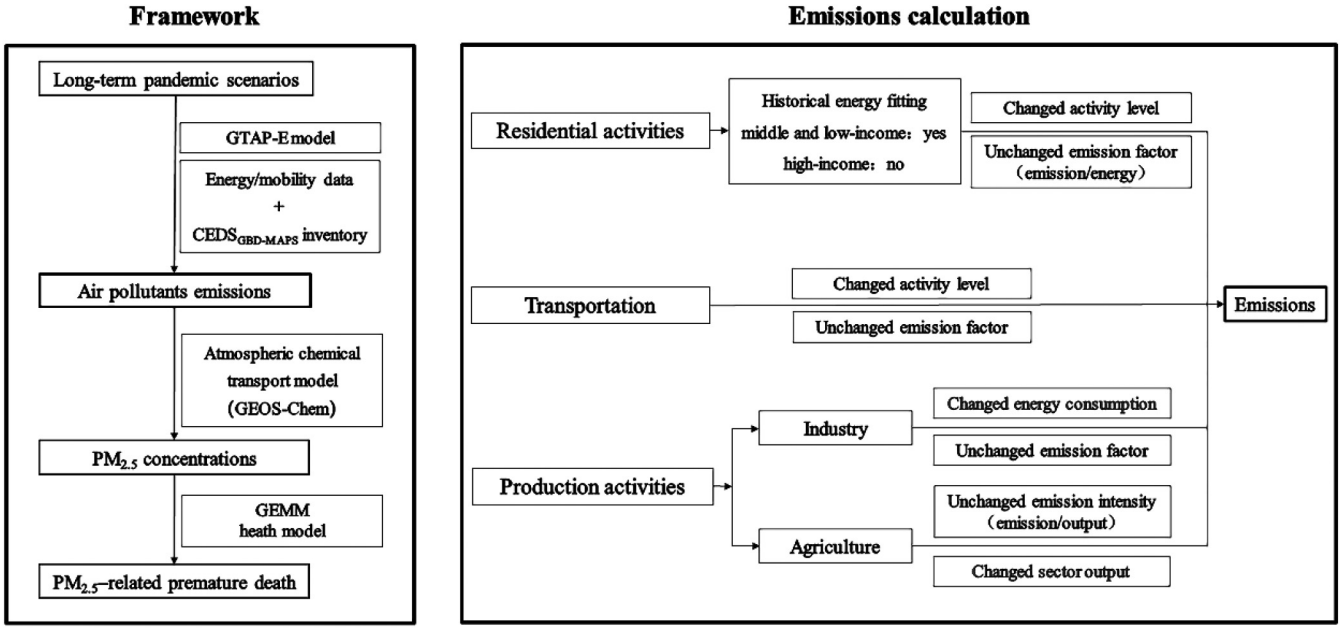

Fig. 1. Methodological framework of this study. The left part presents the framework of the whole study. The right part shows the steps to calculate emission changes in individual sectors under the pandemic scenario.

2.2. Pandemic scenarios

We design two scenarios to estimate the effect of a lasting pandemic. The BASE scenario does not include any pandemics. Here, the economic, energy, emission data and model are based on 2014, which is the latest year with all necessary information available.

The COVID-like scenario denotes a persistent pandemic scenario that mirrors the severity and socioeconomic countermeasures implemented during the first COVID-19 period (the first quarter of 2020 for China and the second quarter for other regions). No fiscal stimuli are included. We assume that the lockdown and other socioeconomic measures remain in place for approximately one year to achieve a new global economic equilibrium state. It is important to note that this duration differs from the actual lockdown period observed during the COVID-19 pandemic.

We consider reductions in labor force, capital and international trade as exogenous shocks to the economy. We collect real employment and gross fixed capital formation data (fixed asset investment for China, due to data limitation) covering over 200 countries in the first COVID-19 period from the CEIC (CEIC dataset, 2022), ILO (International Labor Organization (ILO), 2021) and NBSC (National Bureau of Statistics of China (NBSC), 2021), and then aggregate the data into 31 regions as our shocks setup in GTAP-E. For trade, we assume the same magnitude of increase in trade cost (2.2 % for goods and 6.6 % for services) for all regions, following previous studies (Arriola et al., 2021). The economic effect of trade restrictions is smaller compared with those of labor and capital changes in pandemic cases (Lin et al., 2019; Arriola et al., 2021). Supplementary Table 2 shows the detailed shock settings in GTAP-E for 24 sectors in 31 regions. In addition, we consider the effects of lockdown and weakened economy on transportation, as well as the change in residential activity level as people are required to stay at home. We collect Google (Google, 2020), Apple (Apple, 2020) and Gaode Map (Gaode, 2020) mobility data during the first COVID-19 period to design shocks on transportation mobility and residential activity level (Supplementary Table 3). We also consider affluence-driven changes in residential fuel types.

2.3. The GTAP-E model

We use the GTAP-E to simulate the economic effects and fuel consumption changes of production sectors under a persistent pandemic. The GTAP-E model is an energy-environmental extension of the standard GTAP model, which is a multiregion, multisector, computable general equilibrium (CGE) model (Burniaux and Truong, 2002). After a long history of improvements, CGE is one of the best approaches to analyze economic influences of disasters, new policies and other events. Many studies have used GTAP (Walmsley et al., 2021; Verikios et al., 2016; Verikios et al., 2011) and other CGE models (Dixon et al., 2010; Prager et al., 2017) to assess the economic impacts of pandemics or epidemics. More detailed descriptions about GTAP-E model can be found in Supplementary methods.

The latest version (v10a) of the GTAP database (GTAP v10a Data Base, 2019), which is constructed from the input–output tables of 141 countries and regions across the world with a base year of 2014, is used to build the GTAP-E model in this study. The GTAP database contains 65 sectors and 5 primary production factors. For this study, the 141 countries and regions have been aggregated to 31 regions following our previous studies (Lin et al., 2019; Du et al., 2020). The 65 production sectors are aggregated to a total of 24 sectors (Supplementary data Table 1). Among the 24 sectors, one is the transportation sector, five are agricultural sectors and the remaining 18 are industrial sectors.

2.4. Processing emissions

For all scenarios, natural emissions follow our previous studies (Lin et al., 2019; Du et al., 2020). For anthropogenic emissions, the BASE scenario directly uses the $CEDS_{GBD\text{-}MAPS}$ inventory in the year 2014 for all pollutant types. The $CEDS_{GBD\text{-}MAPS}$ inventory is a newly established global emission dataset for 7 pollutants from 9 fuel types, 57 sectors and 222 countries/regions (McDuffie et al., 2020). More descriptions about the inventory can be found in Supplementary methods. Here we map the 222 regions of $CEDS_{GBD\text{-}MAPS}$ to 141 regions in the original setup of GTAP-E (Supplementary data Table 2), and then to 31 aggregated regions to be consistent with the scenario design.

The land transportation sector in $CEDS_{GBD\text{-}MAPS}$ contains the emissions of both commercial and private vehicles. Commercial vehicles are affected both by direct lockdown measures and the changes in economic production (simulated in GTAP-E). Private vehicles are affected only by the direct lockdown measures. Therefore, we separate emissions of private vehicles from commercial transportation, following the method elsewhere (Lin et al., 2019; Du et al., 2020).

Similarly, the electricity sector in $CEDS_{GBD-MAPS}$ does not separate emissions associated with residential and industrial use. Residential electricity use can change under changed household affluent level and the "stay-at-home" policy, which may be different from the change in industrial electricity use. We regard residential electricity use as part of residential activities that lead to emissions. We extract the emissions associated with residential electricity use from total electricity-related emissions based on the IEA electricity dataset (International Energy Agency (IEA), 2016). The IEA dataset distinguishes electricity consumption by different types of end use (residential, industrial, etc.). For each region, we assume the fraction of residential use to total electricity use to be the residential contribution to total electricity-related emissions. The IEA statistics only covers 85 regions. Thus for a region with no IEA data, the average fraction over its adjacent neighbor regions is used. Supplementary Table 4 shows the fractional contributions of residential electricity in our 31 aggregated regions.

Thus, the emissions associated with residential activities include the residential electricity-related emissions and the emissions in the original $CEDS_{GBD-MAPS}$ residential sector (due to fuel combustion for heating and cooking).

For non-residential sectors, we first map the 56 sectors in $CEDS_{GBD-MAPS}$ to the 65 sectors in the original GTAP-E setup, and then to 24 sectors in our economic shocks setup. The detailed mapping tables are shown in Supplementary data Tables 1 and 3.

2.5. Anthropogenic pollutant emissions for COVID-like scenario

The process of determining anthropogenic emissions in the COVID-like scenario involves the utilization of scenario-specific fuel consumption (or sector outputs) and prescribed emission factors (or emission intensities), which are based on 2014 data (i.e., the BASE scenario).

For the 18 industrial sectors, emissions are derived from scenario-dependent fuel consumption from GTAP-E and unchanged emission factors based on the $CEDS_{GBD-MAPS}$ inventory and energy data. GTAP-E contains three main fossil fuel types (coal, oil and natural gas). $CEDS_{GBD-MAPS}$ contains emissions from nine fuel types; and for the industrial sectors and transportation, most emissions (72 % for BC, 93 % for NOx, 41 % for POA and 78 % for SO_2) are due to combustion of the three fossil fuel types. Therefore, we first aggregate the nine fuel types into five (coal, oil, natural gas, biomass and process). Then for each pollutant, region and industrial sector, we allocate the biomass- and process-related emissions to individual fossil fuels, based on the relative contribution of each fuel type to the total fuel-related emissions. Next, we derive a dataset of emission factors for each pollutant type and fossil fuel type in each of the 18 sectors and 31 regions as the ratio of the respective emissions of 2014 from the $CEDS_{GBD-MAPS}$ inventory divided by the fuel consumption from the IEA energy data. Subsequently, we multiply these emission factor data by the GTAP-E calculated fuel consumption to derive the emissions for individual pollutant types, fossil fuel types, sectors and regions.

For the five agricultural sectors, few fossil fuels are consumed. Thus we assume the fuel structure to be unchanged under the pandemic shocks. For both fuel and non-fuel (especially for NH_3) sources, we follow our previous studies (Lin et al., 2019; Du et al., 2020) to use the constant emission intensities (i.e., emission per unit monetary output) and GTAP-E outputs to calculate anthropogenic emissions under the COVID-like scenario. Specifically, we derive the sector-, region-, and pollutant-specific emission intensities by dividing the emissions of 2014 from the $CEDS_{GBD-MAPS}$ inventory by the outputs from the GTAP database.

For emissions related to transportation, we adopt the percentage changes in route requests from driving during the first COVID-19 period from the Apple Maps Mobility Trend Report (Apple, 2020) as the emission changes for private vehicles. The Apple Report includes 57 countries and takes January 13, 2020 as the baseline. We aggregate data from these regions into 31 regions. The Apple mobility dataset does not contain China, for which country data from the national driving activity index of Gaode Map Travel Report 2020 (Gaode, 2020) are used. For other transportation emissions (commercial land transport, air transport and water transport), we choose as perturbation the larger value of the following two aspects: 1) the GTAP-E simulated economy-driven change in energy consumption for transportation, and 2) the mobility index changes from Apple/Gaode.

As discussed above, residential emissions in this study are contributed by residential electricity use and household fuel combustion. We aggregate the nine fuel types for household fuel combustion in $CEDS_{GBD-MAPS}$ into four (biomass, coal, oil and natural gas); there are no process-related emissions in this sector. Emissions from residential electricity is regarded as another energy type (electricity) here, thus there are totally five energy types in the residential sector. Treatments of residential emissions differ between high-income (per capita gross national income exceeds $12,696 in 2020), middle-income (between $1046 and $12,695) and low-income ($1045 or below) regions; the definition of different affluence groups follows the classification from World Bank and United Nations (United Nations (UN), 2022).

In high-income regions, residential emissions related to energy use (electricity and fuels) are relatively small in BASE. They contribute about 1.4 %–16.7 % of total emissions for most pollutants and 50.1 % for POA. For these high-income regions, we employ the percentage change in residential activity level during the first COVID-19 period based on Google COVID-19 Community Mobility Report (Google, 2020) as a reference to adjust residential emissions. The Google Report includes 114 countries and takes the median value from the 5-week period over January 3–February 6, 2020 to be the baseline to account for the day-of-week effect. We aggregate these regions into 31 regions. The Google mobility data does not include China, thus we take the national time spent indoors changes from Shen et al. (Shen et al., 2021) as our reference. Directly using the value of relative mobility change to adjust residential emissions might lead to an overestimate, because a certain amount of household energy will be consumed no matter people stay at home or go to work. Thus we apply a scaling factor of 0.5 to the mobility change data before using them to calculate residential emission changes.

For middle- and low-income regions, residential energy use is a major emission source. In addition, residential energy structure may change significantly with the affluence level. This effect is accounted for here by applying the historical relationship between affluence and residential energy use. For this purpose, we collect GDP and population data from 2000 to 2014 from two UN datasets. The UN GDP dataset contains 211 regions and the population dataset contains 231 regions, which are mapped to 31 regions to construct per capita GDP as the indicator of affluence. We then fit the historical relationship between per capita GDP and per capita energy consumption for each of the five energy types (electricity, biomass, coal, oil and natural gas) in each region. The fitting is linear or quadratic depending on the characteristics of each region and energy type (Supplementary Fig. 2). The fitted relationships are then applied to the pandemic scenario to obtain residential energy consumption in response to the pandemic-affected affluence level. Residential activity level changes based on Google mobility data/Shen et al. and the scaling factor (0.5) are then applied on top of these energy-specific consumption data to account for the impacts of stay-at-home policies. Finally, energy consumption data are multiplied by energy-specific emission factors to obtain residential emissions under the COVID-like scenario.

2.6. Ambient $PM_{2.5}$ and related premature deaths

To estimate ambient $PM_{2.5}$ concentrations for each scenario, we further aggregate the 31 regions to 13 regions, and apply chemical efficiencies (i.e. annual mean ambient concentration per unit emission) to the emissions in each scenario. The chemical efficiency data have been established by Lin et al. (Lin et al., 2019) and tested in several studies (Chen et al., 2021; Lin et al., 2019; Du et al., 2020) as a low-cost, robust approach to estimate $PM_{2.5}$ concentration. We use region- and pollutant-specific chemical efficiency data to calculate SIOA (from emissions of NOx, SO_2 and NH_3), BC and POA.

We compare the calculated total $PM_{2.5}$ (from all compositions including SIOA, BC, POA, SOA, dusts and sea salts) in BASE with the satellite-derived $PM_{2.5}$ data from van Donkelaar et al. (Van Donkelaar et al., 2016). The population-weighted $PM_{2.5}$ concentrations show good consistency between the two datasets, with R^2 ranging from 0.74 to 1.0 and normalized mean bias from 0.5 % to 10 % across the 13 regions (Supplementary Fig. 3). We further use the biases in BASE to construct scaling factors for each region, and adjust the $PM_{2.5}$ concentrations in each pandemic scenario to eliminate the systematic error, following our previous studies (Lin et al., 2019; Du et al., 2020).

We employ the GEMM model (Burnett et al., 2018) to estimate premature deaths due to long-term exposure to ambient $PM_{2.5}$. The GEMM method addresses many limitations of previous Integrated Exposure-Response (IER) model (Burnett et al., 2018). Both GEMM and IER consider five individual causes of mortality, including ischemic heart disease, stroke, chronic obstructive pulmonary disease, lung cancer, and lower respiratory infections. GEMM offers another accounting method combining all noncommunicable diseases and lower respiratory infections (LRIs), which is used in our main text (referred to as GEMM NCD + LRI). The detailed calculation process can be found in our previous study (Lin et al., 2019). In order to assess the impact of using different methods, we conduct a comparative analysis for 13 individual regions under two scenarios based on GEMM 5COD (based on five individual causes), GEMM NCD + LRI and IER. The results are presented in Supplementary data Tables 4 and 5. Supplementary data Table 6 compares our global mortality estimates in the BASE scenario (which represents the actual situation in 2014) with those reported by Burnett et al. (Burnett et al., 2018). Our results show a slight difference of 22 %, which is consistent with the findings of Lin et al. (Lin et al., 2019) (20 %). The difference is attributable to our use of an updated version of baseline mortality data and a grid cell-based calculation approach. Specifically, we compute the mortality for each discrete grid cell by considering their respective $PM_{2.5}$ concentrations, rather than applying the national mean $PM_{2.5}$ concentration.

2.7. Uncertainty estimates

The uncertainties of our study come from a few sources. First, the GTAP-E model simulates the economic states at equilibrium rather than the dynamic economic evolution. The model parameters and structure also contain uncertainties to various extents. We change six main parameters by ± 50 % to quantify the uncertainties related to model parameters. Globally, the 50 % changes cause the GDP change by -0.17 % to 0.04 % (Supplementary data Table 7), suggesting that the simulation results are robust to parameter variation. We also compare the modeled economic changes under the COVID-like scenario with the actual statistics for the first COVID-19 period. The results show slight differences (globally 0.12 %), indicating good model performance.

Second, estimates of air pollutant emissions are affected by errors in emission factors and activity data, as discussed in detail for $CEDS_{GBD\text{-}MAPS}$ (McDuffie et al., 2020). Emission errors for 13 regions are estimated in previous studies (Lin et al., 2016; Zhang et al., 2017). For scenario-dependent $PM_{2.5}$ concentrations and health impact calculations, the emission errors are implicit in the derivation of σ4 below.

Third, we assume that for a given pollutant, region, sector and fuel type, the emission factor remains unchanged for all scenarios, and for the agricultural sectors, the emission intensity for a given pollutant, region and sector remains unchanged. This may lead to an additional uncertainty in the calculated emissions for the pandemic scenarios, which is assumed to be $\sigma 1 = 5\%$ (one standard deviation).

Fourth, we adopt the statistical relationships fitted from historical data to calculate residential energy consumption caused by economic downturn in middle- and low-income regions. We use the normalized root-mean-square deviation (NRMSD) between the fitted results and the actual per capita fuel consumption data over 2000–2014 to represent the overall fitting errors for each region and energy type. For high-income regions, we assume the residential energy structure remains unaffected by the pandemic, and assume the associated error to be 10 %. The error is referred to as σ2 (one standard deviation).

Fifth, we use the statistics for the changes in residential activity and transportation mobility for the first COVID period to adjust/scale emissions of the residential and transportation sectors. This activity-level-based adjustment might introduce uncertainty in the calculation of emissions. This uncertainty source is referred to as σ3 (one standard deviation) with an assumed value of 20 %.

Sixth, there are two uncertainty sources with respect to the use of chemical efficiencies. One error source is from imperfect GEOS-Chem simulations to construct the chemical efficiencies, and is referred to as σ4 (one standard deviation). The other error source is related to the application of chemical efficiencies to each pandemic scenario, and is referred to as σ5 (one standard deviation). Following our previous studies (Lin et al., 2019; Du et al., 2020), we use the NRMSD between calculated and satellite-derived population-weighted $PM_{2.5}$ concentrations as σ4 and assume $\sigma 5 = 15\%$.

Seventh, the uncertainty associated with GEMM pollution exposure-response calculations is represented by 95 % CI of the mortality results by changing the GEMM model parameters. This error, when expressed as one standard deviation, is referred to as σ6. Although there may be synergistic health effects of the virus and the $PM_{2.5}$ pollution (Wu et al., 2020; Conticini et al., 2020), these synergistic effects are not accounted for here due to lack of concrete evidence (Walton et al., 2021).

The overall uncertainty in premature deaths for each pandemic scenario is estimated as the sum in quadrature of the above error terms. Errors are expressed as 95 % CI in the main text. Although σ4 and σ6 are major sources of uncertainty, they are subject to causes that do not depend on the scenario. Thus, σ4 and σ6 are not relevant when discussing the relative change in premature mortality from one scenario to another.

3. Results and discussion

3.1. Economic response to a persisting pandemic

We first assess the economic effect of a persisting COVID-like pandemic using the GTAP-E model. We consider three main exogenous variables of the modeled economy perturbed by the pandemic, including labor, capital and trade cost. We focus on the economic responses without fiscal stimuli. During the lockdown time, many industries are closed and people are forced to stay at home for social distancing, leading to a dramatic reduction in labor working hours (Organization, 2020). Capital investment is reduced due to a worsened economic prospect (UNCTAD, 2020). Trade restrictions are also strengthened in order to reduce virus spread (UNCTAD, 2020). The GTAP-E model results show that due to the pandemic, the global gross domestic product (GDP) declines by 10.9 %, of which 10.2 % is caused by the decreases in capital and labor together.

There are substantial inter-regional differences in the simulated economic impacts of the pandemic (Fig. 2a). Here we aggregate the economic results of 31 regions into 13 regions to be consistent with the following environmental analysis. In general, less affluent regions tend to suffer larger fractional economic losses than more affluent regions do. For example, the GDP declines in South Asia (24.8 %) and Sub-Sahara Africa (18.9 %) are much larger than those in the United States (10.9 %) and Oceania (Australia and New Zealand, 5.7 %). This is mainly because the economic systems of less affluent regions tend to be more fragile and subject to larger capital losses caused by the pandemic (Supplementary Table 2).

There are uncertainties in the economic simulation related to model structure and parameters. We quantify the uncertainties by conducting two sensitivity tests including six main parameters: elasticity of substitution in value-added-energy subproduction, capital-energy subproduction, energy subproduction, non-electricity energy subproduction and non-coal energy subproduction, and Armington CES for domestic/imported allocation. Increasing or decreasing the parameters by 50 % caused the global GDP to change by -0.17 % to 0.04 %, with the highest percentage change observed in India (-2.19 % to 0.76 %). Results and tests are detailed in

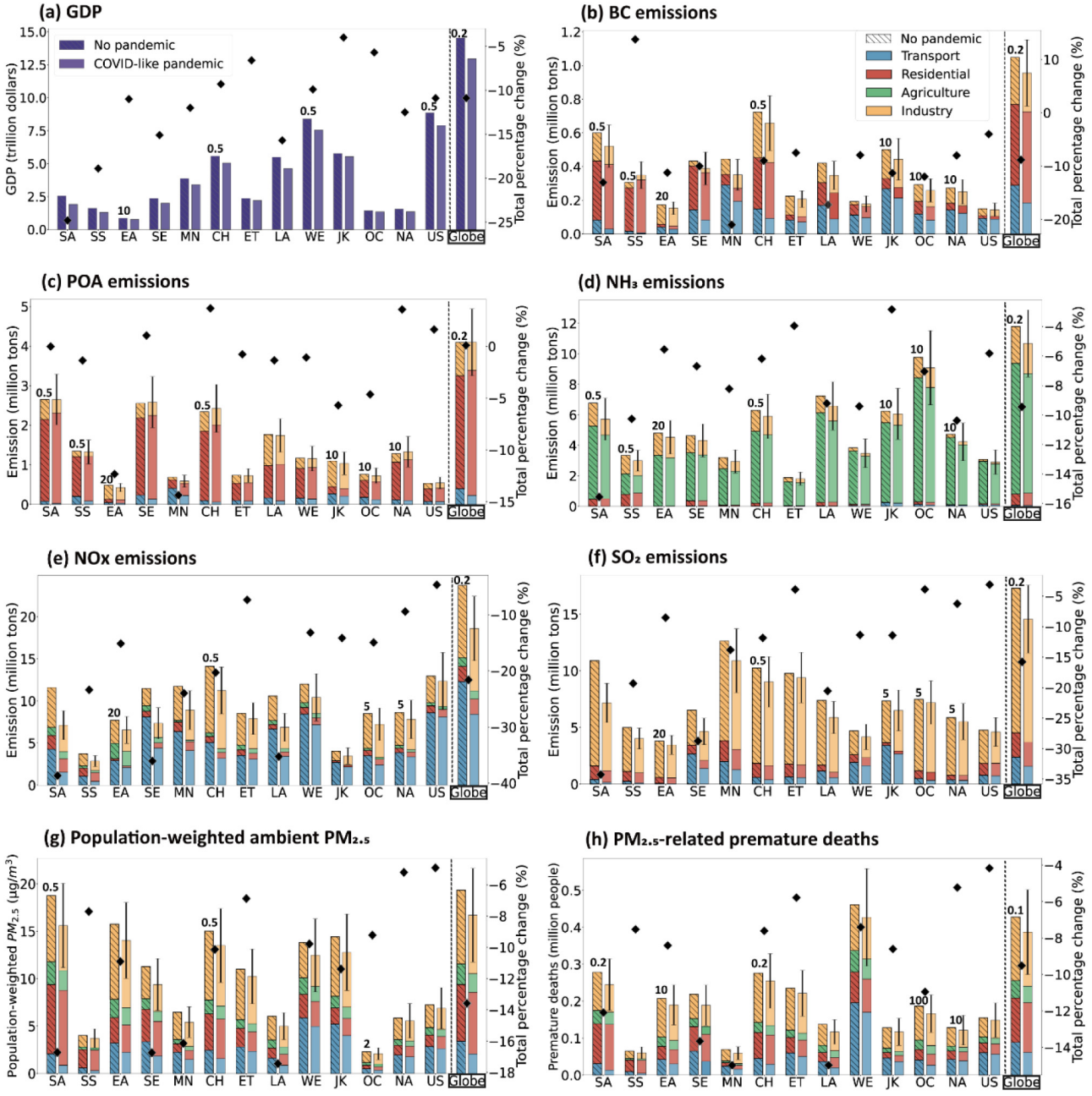

Fig. 2. Economic and environmental impacts of a persisting COVID-like pandemic. The figure shows the GDP, anthropogenic pollutant emissions, population-weighted $PM_{2.5}$ concentrations and related premature deaths in 13 regions with and without the COVID-like pandemic. Here, $PM_{2.5}$ concentrations and related premature deaths are contributed by anthropogenic SIOA, BC and POA. For some regions, results are scaled for better presentation, with the scaling factors indicated on the top of the bars denoting the no pandemic case. Error bars denote the uncertainty ranges (95 % CI) due to the assumption of unchanged emission factor/intensity, the statistical calculation of affluence-related residential energy use, and the use of mobility data and chemical efficiencies; common error sources among different scenarios are not included here. The black points denote the percentage changes. Thirteen regions include China (CH), rest of East Asia (EA), Economies in Transition (ET), Japan and Korea (JK), Latin America and Caribbean (LA), Middle East and North Africa (MN), Rest of North America (NA), Oceania (OC), South Asia (SA), South-East Asia and Pacific (SE), Sub-Saharan Africa (SS), the United States (US), and Western Europe (WE). The regions are sorted from the least to the most affluent region according to per capita GDP (from left to right).

Supplementary data Tables 7 and 8. We then compare the GTAP-E economic results with the actual year-on-year GDP change data for the first COVID-19 period (i.e., from 2019 to 2020, for the first quarter in China and the second quarter in other regions), which roughly reflect the effect of COVID-19 in the absence of economic stimuli (Supplementary Fig. 4). Overall, the simulated GDP declines are consistent with the actual statistics, including the global GDP decline (-10.9 % versus -11.0 %) and the respective inter-regional differences. The global difference is within the uncertainty caused by model parameters. Furthermore, GTAP-E simulates the GDP change between equilibriums, whereas the actual GDP data may reflect a transitional economic change from 2019 to 2020.

3.2. Changes in emissions and pollution

Under the persisting COVID-like pandemic, anthropogenic air pollutant emissions change greatly, but the sign and magnitude of emission changes differ across the pollutants and regions (Fig. 2b–f). For NH_3, SO_2 and NOx, the global total emissions decrease by 9.5 % (5.6 million tons), 15.8 % (13.6

million tons) and 21.6 % (25.6 million tons), respectively. Less affluent regions tend to exhibit greater fractional emission reductions than more affluent regions do for SO_2 and NOx, although with notable data scatter. In particular, South Asia and Sub-Sahara Africa exhibit SO_2 emission reductions by 34.3 % and 19.3 %, respectively, whereas the United States only has a weak decline (3.1 %) (Fig. 2f). This is because SO_2 and NOx emissions are mainly coming from industry (for both) and transportation (for NOx), which experience greater declines in less affluent regions. Transportation emissions of NOx decrease by 34.7 % globally and by up to 64.0 % in South Asia and 48.4 % in Latin America and Caribbean. The NH_3 emission result is broadly consistent with the GDP result, because the pollutant is emitted mainly from the agricultural sectors directly producing GDP (Fig. 2d). For NH_3, SO_2 and NOx, residential fuel use is a minor emission source, and residential emission changes only have small effects on their total emissions. Our estimated emission changes are consistent with previous studies on COVID-19 (Keller et al., 2021; Bauwens et al., 2020; Zheng et al., 2020; Venter et al., 2020) – for example, Chinese NOx emissions decrease by 20.4 % here and by about 20 % from the first quarter of 2019 to the same time of 2020 in ref. (Zheng et al., 2020); and global NOx emissions decrease by 21.6 % here, comparable to the 18 % reduction in ambient concentration in ref. (Keller et al., 2021).

In contrast, global total anthropogenic POA emission increases negligibly (by 0.1 % or 0.02 million tons) in response to the pandemic (Fig. 2c). This is because the reductions in industrial and transportation emissions are offset by the increases in residential emissions. As a major source of POA, residential emissions increase in part because residential activities exhibit a global average increase of 7.2 % due to longer stay-at-home time. Furthermore, the estimated switch of residential energy use from cleaner to cheaper but more polluting energy types associated with reduced affluence is notable in less affluent regions. For example, in Middle East and North Africa and Latin America and Caribbean, residential electricity use decreases by 17 % and 18 %, respectively, whereas residential biomass increases by 26 % and 4.1 % in the meantime. This affluence-dependent emission estimate is supported by the analysis of historical household energy use – as per capita GDP increases, consumption of cheap but most polluting fuel (biomass) decreases while cleaner but expensive energy (electricity and gas) increases in general (Supplementary Fig. 2). Regionally, Middle East and North Africa and East Asia exhibit the greatest fractional decreases of total POA emissions (14.4 % and 12.3 %, respectively) due to substantial declines in industrial and transportation activities. In contrast, China exhibits the greatest fractional POA emission rise by 3.7 %, followed by Rest of North America (mainly Canada, 3.6 %).

BC emissions exhibit a global average reduction by 8.8 % in response to the pandemic, but with large regional diversity. Globally, the increase in residential emissions only partially offset the decreases in industrial and transportation emissions. The residential contribution to total BC emission is dominant in least affluent regions, whereas industry is the main source for more affluent regions (Fig. 2b). The residential contribution is greatest (83.9 %) in Sub-Sahara Africa, which is also the only region exhibiting a significant increase in total BC emission by 13.8 %. In contrast, BC emissions decrease most in the Middle East and North Africa (by 21.0 %), followed by Latin America and Caribbean (17.3 %) and South Asia (13.1 %).

We then estimate the changes in ambient $PM_{2.5}$ concentrations caused by the persisting COVID-like pandemic. Fig. 3 shows that BC concentrations increase slightly over Sub-Saharan Africa but decrease at other places as a result of the pandemic-induced changes in pollutant emissions. By comparison, POA concentrations increase slightly over several Asian regions and North America, but with declines over other areas. SIOA concentrations decrease greatly worldwide with the most notable reductions in absolute value over China and India. Summing over the changes in BC, POA and SIOA, the changes in total $PM_{2.5}$ are negative with a global average decline by 2.3 $\mu g/m^3$ over regions with population densities exceeding 100/km^2. Fig. 2g further shows the large fractional decline in population-weighted global average $PM_{2.5}$ (sum of BC, POA and SIOA) concentrations (13.6 %) with substantial regional differences (from 4.9 % to 17.4 %).

We compare our $PM_{2.5}$ concentration results with the actual year-on-year change for the first COVID-19 period over the 13 regions. The actual data are taken as the average of values from the World Air Quality Index project (The World Air Quality Index Project (WAQI), 2022) (after conversion from daily medium values of Air Quality Index to concentrations) and the satellite-derived $PM_{2.5}$ dataset (van Donkelaar et al., 2021). Supplementary Fig. 5 shows that our estimated $PM_{2.5}$ concentration changes for the 13 regions are consistent with those shown in the actual data with slope of 1.2 and R^2 of 0.86, in support of the credibility of our estimated $PM_{2.5}$ changes.

Fig. 2h further shows the changes in $PM_{2.5}$-related (sum of BC, POA and SIOA) premature mortality caused by the persisting COVID-like pandemic. Globally, the cases of premature death decrease by 0.41 [95 % CI: 0.34–0.47] million, with a relative change by −9.5 %. The number of cases is equivalent to 80 % of the mortality cases recorded to be directly caused by COVID-19 in the first COVID period (World Health Organization (WHO), 2022). Regional differences in mortality changes are also substantial. South Asia exhibits the largest number of mortality reduction by 0.17 million (12.1 %), followed by China (0.11 million, 7.6 %) and Western Europe (0.03 million, 7.4 %). Latin America exhibits the greatest fractional mortality reduction by 15.0 % while the United States experiences the smallest fractional reduction by 4.2 %.

3.3. Environmental inequality

Contrasting the regional changes in GDP and population-weighted $PM_{2.5}$ concentrations or related mortality reveals exacerbated environmental inequality as a result of the pandemic. The blue dots in Fig. 4 show that the fractional changes in $PM_{2.5}$ concentrations (sum of BC, POA and SIOA) and associated mortality are notably larger than the changes in GDP for Oceania, Japan and Korea, and Middle East and North Africa. In contrast, the opposite result is true for South Asia, Sub-Sahara Africa, the United States and North America. South Asia and Sub-Sahara Africa, the least affluent of the 13 regions, suffer 24.8 % and 18.9 % losses respectively in GDP but with much weaker extents of pollution-associated mortality alleviation (12.1 % and 7.5 %). This is mainly caused by the changes in residential energy use.

The global population-weighted average $PM_{2.5}$ concentration (sum of BC, POA and SIOA) is reduced by the pandemic by 2.6 $\mu g/m^3$, as a result of the reduction associated with non-residential sectors (3.1 $\mu g/m^3$) partly compensated by the enhancement associated with the residential sector (0.5 $\mu g/m^3$). Thus, including the residential response increases the global $PM_{2.5}$-related mortality by 3.5 % (from −13.0 % to −9.5 %; orange versus blue dots in Fig. 4). Of this global mortality change, switch to more polluting household energy types contributes 37 %, with the remaining contributed by longer stay-at-home time requiring more household energy consumption. Affluent regions exhibit small fractional changes in mortality when the residential response is included, like Oceania (0.7 %) and the United States (1.3 %). In contrast, less affluent regions exhibit substantial mortality enhancements with the inclusion of residential response, especially for Sub-Saharan Africa (6.4 %) and South Asia (5.6 %). These results are because in less affluent regions, as compared to more affluent ones, residential emissions are a more important pollution source and are subject to more significant changes by the pandemic. Thus the changes in residential emissions largely determine the extent of economic-pollution consistency in their responses to the pandemic.

3.4. Call to mitigate inequality

Our results show that considering the full chain of changes in economy, affluence and household energy use in response to a persisting pandemic, the fractional decline in $PM_{2.5}$-related (sum of BC, POA and SIOA) mortality is close to the GDP decline at the global level. Regionally, however, the economic-environmental contrast is exacerbated, as a few least affluent regions suffer the largest fractional economic losses with no comparable levels of alleviation in pollution and related mortality. This is because affluence-dependent residential pollution increases to partly offset the effect of emission reductions in other sectors.

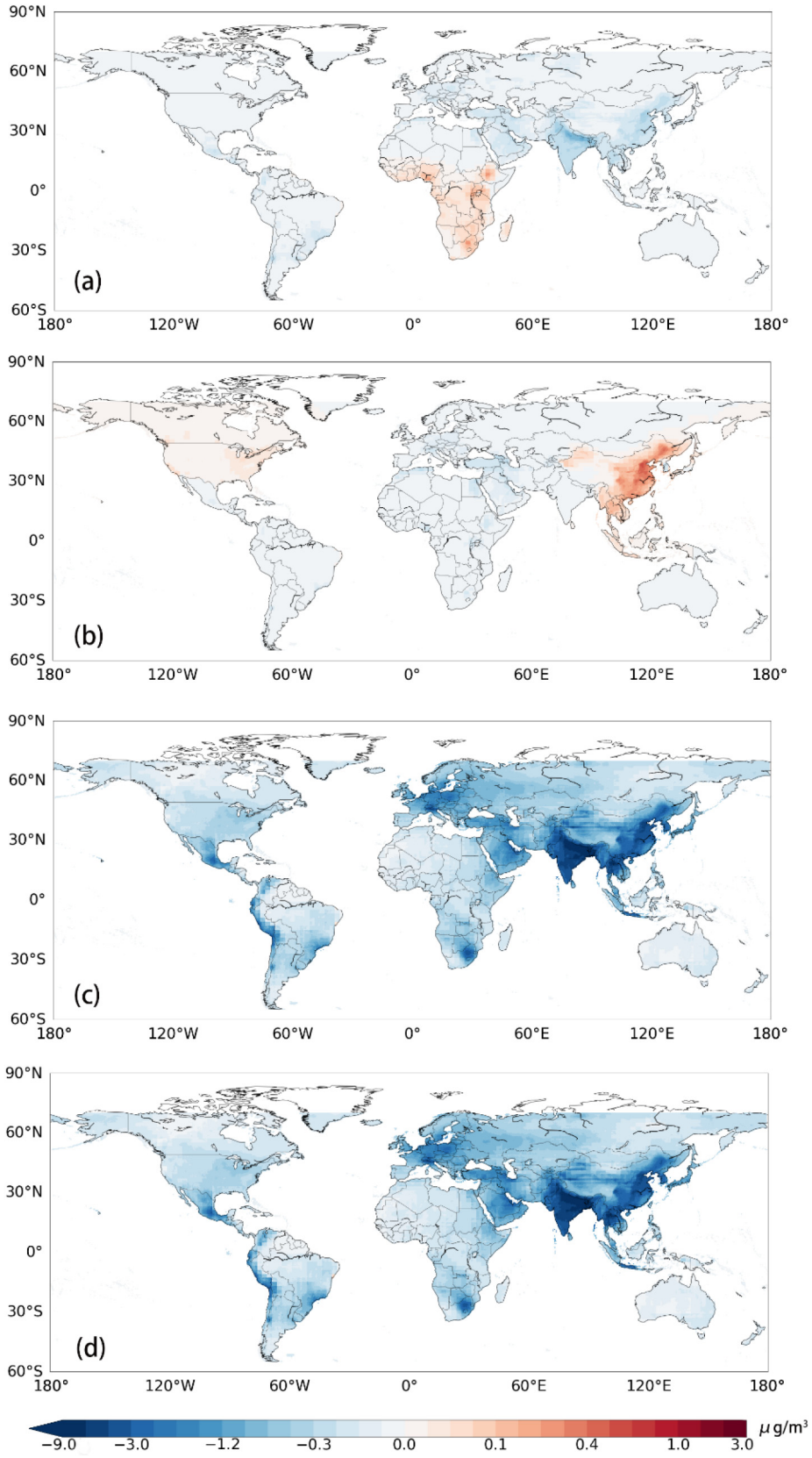

Fig. 3. Pollution impacts of pandemic. The simulated geographical distributions of changes in BC (a), POA (b), SIOA (c) and total $PM_{2.5}$ concentrations (d) under the persisting COVID-like pandemic. The color scales are nonlinear.

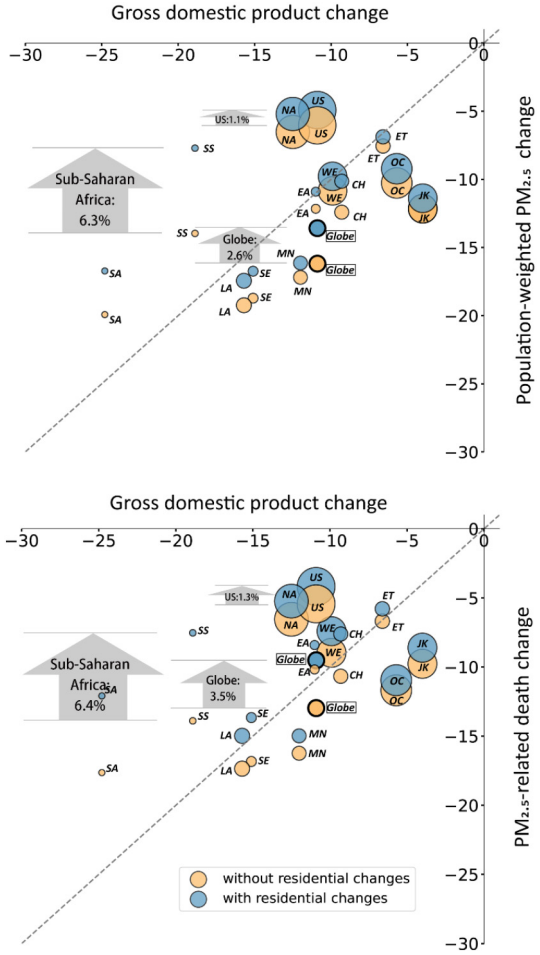

Fig. 4. Contrast between pandemic caused economic and pollution changes. The figure shows the percentage changes in regional population-weighted $PM_{2.5}$ concentrations and related premature mortality as a function of the percentage changes in GDP caused by the COVID-like pandemic. Blue dots denote the regional results including the changes in all anthropogenic emission sectors, and orange dots denote the results excluding the changes in the residential sector. The size of each dot denotes the magnitude of per capita GDP in each region. The dots with a darker color and thicker border denote the global values. The gray arrows show the differences between the percentage changes including and excluding the residential sector for the United States, Sub-Saharan Africa and global average. Thirteen regions include China (CH), rest of East Asia (EA), Economies in Transition (ET), Japan and Korea (JK), Latin America and Caribbean (LA), Middle East and North Africa (MN), rest of North America (NA), Oceania (OC), South Asia (SA), South-East Asia and Pacific (SE), Sub-Saharan Africa (SS), the United States (US), and Western Europe (WE). The gray dotted line represents the 1:1 line.

This study does not include the effect of fiscal stimulus. Affluent regions have the capability to implement large-scale fiscal stimuli, which reduce the economic and pollution changes caused by the pandemic. The least affluent regions are also least capable to implement strong fiscal stimuli. Thus including the effect of fiscal stimuli (in affluent regions) would increase the calculated inter-regional economic inequality. Furthermore, this study does not consider indoor $PM_{2.5}$ pollution, which would further worsen the inter-regional health inequality. This is because indoor pollution from residential fuel combustion can be a larger health threat than ambient pollution in less affluent regions (Shen et al., 2021; Yun et al., 2020; Mbandi, 2020; Giwa et al., 2019), and longer time to stay at home and switch to more polluting household fuel types would mean enhanced exposure to indoor pollution (Shen et al., 2021; Li et al., 2021).

The key to reducing the pandemic-caused inter-regional environmental inequality and protecting lives worldwide lies in swift lockdown measures to minimize infection spread, timely invention and taking of effective vaccines, and international financial, technological and vaccine aids to least affluent regions. In addition to local efforts, time-efficient international aids are crucial, as the least affluent regions have already struggled to afford clean energy even without the pandemic (British Petroleum Company, 2019; International Energy Agency (IEA), 2016), and the pandemic further worsens the situation (Mbandi, 2020). For example, electricity is not available for about 600 million households and over 900 million rely heavily on polluting energy for cooking in Africa (IEA, 2019). Aids to mitigate pollution in these regions will also have global health benefits by reducing the atmospheric transport of pollutants (Chen et al., 2021; Zhang et al., 2017).

CRediT authorship contribution statement

J.L. conceived the research. J.L. and C.L. designed the research. C.L. performed the research. C.L. and J.L. designed the scenarios. E.M. provided emission data. Q.C. and Y.L. helped C.L. to perform the economic simulations. C.L. calculated emissions and health impacts. L.C. performed atmospheric simulations and calculated chemical efficiencies. J.L. and C.L led the analysis with inputs from C.L., K.H., M.D., Q.C., Y.L. and J.W. And C.L. and J.L. wrote the manuscript. All authors discussed commented on the manuscript.

Data availability

Data will be made available on request.

Declaration of competing interest

The authors declare that they have no conflict of interest.

Acknowledgment

We thank Randall Martin for information of satellite-based $PM_{2.5}$ data, Shu Tao and Xiao Yun for discussion of residential response. This study is supported by the National Natural Science Foundation of China (42075175, 72125010, 72243011 and 71974186).

Appendix A. Supplementary data

Supplementary data to this article can be found online at https://doi.org/10.1016/j.scitotenv.2023.163191.

References

Apple, 2020. Apple Maps MobilityTrends Report. Available at. https://covid19.apple.com/mobility.

Arriola, C., Kowalski, P., Smith, D., van Tongeren, F., 2021. Analysing the impact of COVID-19 on the global economy. Available at https://www.gtap.agecon.purdue.edu/resources/download/10486.pdf.

Bauwens, M., et al., 2020. Impact of coronavirus outbreak on NO2 pollution assessed using TROPOMI and OMI observations. Geophys. Res. Lett. 47, e2020GL087978. https://doi.org/10.1029/2020GL087978.

Boden, T., Marland, G., Andres, R., 2017. Global, Regional, and National Fossil-Fuel CO2 Emissions. Carbon Dioxide Information Analysis Center, Oak Ridge National Laboratory. US Department of Energy, Oak Ridge, Tenn., USA 2009 https://doi.org/10.3334/CDIAC1.

British Petroleum Company, 2019. BP Statistical Review of World Energy. Available at https://www.bp.com/content/dam/bp/businesssites/en/global/corporate/pdfs/energy-economics/statistical-review/bp-stats-review-2019-full-report.pdf.

Burnett, R., et al., 2018. Global estimates of mortality associated with long-term exposure to outdoor fine particulate matter. Proc. Natl. Acad. Sci. 115, 9592–9597.

Burniaux, J.-M., Truong, T.P., 2002. GTAP-E: an energy-environmental version of the GTAP model. GTAP Technical Papers. 18.

CEIC dataset, 2022. . Available at https://www.ceicdata.com/en.

Chen, L., et al., 2021. Inequality in historical transboundary anthropogenic PM2.5 health impacts. Sci.Bull. https://doi.org/10.1016/j.scib.2021.11.007.

Chen, Y., et al., 2018. Estimating household air pollution exposures and health impacts from space heating in rural China. Environ. Int. 119, 117–124.

Conticini, E., Frediani, B., Caro, D., 2020. Can atmospheric pollution be considered a co-factor in extremely high level of SARS-CoV-2 lethality in Northern Italy? Environ. Pollut. 261, 114465.

Dixon, P.B., et al., 2010. Effects on the US of an H1N1 epidemic: analysis with a quarterly CGE model. J. Homel. Secur. Emerg. Manag. 7.
Du, M., et al., 2020. Winners and losers of the Sino–US trade war from economic and environmental perspectives. Environ. Res. Lett. 15, 094032. https://doi.org/10.1088/1748-9326/aba3d5.
Elavarasan, R.M., et al., 2020. COVID-19: impact analysis and recommendations for power sector operation. Appl. Energy 279, 115739.
Fernandes, S.D., Trautmann, N.M., Streets, D.G., Roden, C.A., Bond, T.C., 2007. Global biofuel use, 1850–2000. Glob. Biogeochem. Cycles 21.
Forster, P.M., et al., 2020. Current and future global climate impacts resulting from COVID-19. Nat. Clim. Chang. 10, 913–919. https://doi.org/10.1038/s41558-020-0883-0.
Gaode, 2020. Gaode Map Travel Report 2020: national driving activity index. Available at https://report.amap.com/index.do.
GEOS-Chem v11-01, 2017. . Available at http://wiki.seas.harvard.edu/geos-chem/index.php/Main_Page.
Giwa, S.O., Nwaokocha, C.N., Odufuwa, B.O., 2019. Air pollutants characterization of kitchen microenvironments in southwest Nigeria. Build. Environ. 153, 138–147.
Google, 2020. Google LLC Community Mobility Reports. Available at. https://www.google.com/covid19/mobility/.
GTAP v10a Data Base, 2019. . Available at https://www.gtap.agecon.purdue.edu/databases/v10/index.aspx.
Hammer, M.S., et al., 2021. Effects of COVID-19 lockdowns on fine particulate matter concentrations. Sci. Adv. 7, eabg7670.
He, G., Pan, Y., Tanaka, T., 2020. The short-term impacts of COVID-19 lockdown on urban air pollution in China. Nat.Sustain. 3, 1005–1011.
Hook, A., Sovacool, B.K., Sorrell, S., 2020. A systematic review of the energy and climate impacts of teleworking. Environ. Res. Lett. 15, 093003.
Huang, X., et al., 2021. Enhanced secondary pollution offset reduction of primary emissions during COVID-19 lockdown in China. Natl. Sci. Rev. 8, nwaa137.
Huber, I., et al., 2020. Symposium report: emerging threats for human health–impact of socio-economic and climate change on zoonotic diseases in the republic of Sakha (Yakutia), Russia. Int. J. Circumpolar Health 79, 1715698.
Hueffer, K., Drown, D., Romanovsky, V., Hennessy, T., 2020. Factors contributing to Anthrax outbreaks in the circumpolar north. EcoHealth 17, 174–180.
IEA, 2019. IEA (International Energy Agency) Africa Energy Outlook 2019 World Energy Outlook Special Report. Available atEA Publications. www.iea.org/t&c/.
International Energy Agency (IEA), 2016. World Energy Statistics. Available at. http://www.iea.org/statistics/.
International Labor Organization (ILO), 2021. Statistics and databases. Available at https://www.ilo.org/global/statistics-and-databases/lang–en/index.htm.
Keller, C.A., et al., 2021. Global impact of COVID-19 restrictions on the surface concentrations of nitrogen dioxide and ozone. Atmos. Chem. Phys. 21, 3555–3592.
Kikstra, J.S., et al., 2021. Climate mitigation scenarios with persistent COVID-19-related energy demand changes. Nat. Energy https://doi.org/10.1038/s41560-021-00904-8.
Lake, R.W., 1996. Volunteers, NIMBYs, and environmental justice: dilemmas of democratic practice. Antipode 28, 160–174.
Le, T., et al., 2020. Unexpected air pollution with marked emission reductions during the COVID-19 outbreak in China. Science 369, 702–706.
Lee, J.D., Drysdale, W.S., Finch, D.P., Wilde, S.E., Palmer, P.I., 2020. UK surface NO 2 levels dropped by 42% during the COVID-19 lockdown: impact on surface O 3. Atmos. Chem. Phys. 20, 15743–15759.
Lelieveld, J., Evans, J.S., Fnais, M., Giannadaki, D., Pozzer, A., 2015. The contribution of outdoor air pollution sources to premature mortality on a global scale. Nature 525, 367–371.
Li, J., et al., 2021. Field-based evidence of changes in household PM2. 5 and exposure during the 2020 national quarantine in China. Environ. Res. Lett. 16, 094020.
Lin, J., et al., 2016. Global climate forcing of aerosols embodied in international trade. Nat. Geosci. 9, 790–794.
Lin, J., et al., 2019. Carbon and health implications of trade restrictions. Nat. Commun. 10, 4947. https://doi.org/10.1038/s41467-019-12890-3.
Mackenbach, J.P., Kunst, A.E., Cavelaars, A.E., Groenhof, F., Geurts, J.J., 1997. Socioeconomic inequalities in morbidity and mortality in western Europe. Lancet 349, 1655–1659.
Mahato, S., Pal, S., Ghosh, K.G., 2020. Effect of lockdown amid COVID-19 pandemic on air quality of the megacity Delhi,India. Sci. Total Environ. 139086.
Marani, M., Katul, G.G., Pan, W.K., Parolari, A.J., 2021. Intensity and frequency of extreme novel epidemics. Proc. Natl. Acad. Sci. 118.
Mbandi, A.M., 2020. Air pollution in Africa in the time of COVID-19: the air we breathe indoors and outdoors. Clean Air J. 30, 1–3.
McDuffie, E.E., et al., 2020. A global anthropogenic emission inventory of atmospheric pollutants from sector-and fuel-specific sources (1970–2017): an application of the community emissions data system (CEDS). Earth Syst.Sci.Data 12, 3413–3442.
National Bureau of Statistics of China (NBSC), 2021. Statistical Database. Available at http://www.stats.gov.cn/english/.
Organization, I.L., 2020. ILO Monitor: COVID-19 and the World of Work.
Prager, F., Wei, D., Rose, A., 2017. Total economic consequences of an influenza outbreak in the United States. Risk Anal. 37, 4–19.
Shen, H., et al., 2021. Increased air pollution exposure among the Chinese population during the national quarantine in 2020. Nat. Hum. Behav. 5, 239–246.
Szasz, A., Meuser, M., 1997. Environmental inequalities: literature review and proposals for new directions in research and theory. Curr. Sociol. 45, 99–120.
Tao, S., et al., 2018. Quantifying the rural residential energy transition in China from 1992 to 2012 through a representative national survey. Nat. Energy 3, 567–573.
The World Air Quality Index Project (WAQI), 2022. . Available at https://aqicn.org/data-platform/covid19/.
UNCTAD, 2020. United Nations Conference on Trade and Development (UNCTAD),Trade and Development Report 2020. Available at. https://unctad.org/publication/trade-and-development-report-2020.
United Nations (UN), 2022. World economic situation and prospects. Available at https://www.un.org/zh/node/164995.
Van Donkelaar, A., et al., 2016. Global estimates of fine particulate matter using a combined geophysical-statistical method with information from satellites, models, and monitors. Environ.Sci.Technol. 50, 3762–3772.
van Donkelaar, A., et al., 2021. Monthly global estimates of fine particulate matter and their uncertainty. Environ.Sci.Technol. 55, 15287–15300.
Venter, Z.S., Aunan, K., Chowdhury, S., Lelieveld, J., 2020. COVID-19 lockdowns cause global air pollution declines. Available atProc. Natl. Acad. Sci. 117, 18984–18990.
Verikios, G., Sullivan, M., Stojanovski, P., Giesecke, J., Woo, G., 2011. The Global Economic Effects of Pandemic Influenza. Available at: https://vuir.vu.edu.au/29271/1/g-224.pdf.
Verikios, G., Sullivan, M., Stojanovski, P., Giesecke, J., Woo, G., 2016. Assessing regional risks from pandemic influenza: a scenario analysis. World Econ. 39, 1225–1255.
Walmsley, T.L., Rose, A., Wei, D., 2021. Impacts on the US macroeconomy of mandatory business closures in response to the COVID-19 Pandemic. Appl. Econ. Lett. 28, 1293–1300.
Walton, H., Kasdagli, D.E.M., Selley, L., Dajnak, D., Katsouyanni, K., 2021. Investigating the links between air pollution, COVID-19 and lower respiratory infectious diseases. Available at https://www.imperial.ac.uk/school-public-health/environmental-research-group/research/air-pollution-epidemiology/air-pollution-and-covid-19/.
Watts, N., et al., 2018. The Lancet Countdown on health and climate change: from 25 years of inaction to a global transformation for public health. Lancet 391, 581–630.
Williams, D.R., Collins, C., 1995. US socioeconomic and racial differences in health: patterns and explanations. Annu. Rev. Sociol. 21, 349–386.
World Health Organization (WHO), 2020. Coronavirus disease 2019 (COVID-19): situation report. Available at: https://apps.who.int/iris/handle/10665/331475 https://covid19.who.int/.
World Health Organization (WHO), 2022. Coronavirus (COVID-19) Data. Available at https://covid19.who.int/data.
Wu, X., Nethery, R.C., Sabath, B.M., Braun, D., Dominici, F., 2020. Exposure to Air Pollution and COVID-19 Mortality in the United States MedRxiv.
Yun, X., et al., 2020. Residential solid fuel emissions contribute significantly to air pollution and associated health impacts in China. Sci. Adv. 6, eaba7621.
Zhang, Q., et al., 2017. Transboundary health impacts of transported global air pollution and international trade. Nature 543, 705–709.
Zhang, W., et al., 2018. Revealing environmental inequality hidden in China's inter-regional trade. Environ.Sci.Technol. 52, 7171–7181.
Zheng, B., et al., 2020. Satellite-based estimates of decline and rebound in China's CO2 emissions during COVID-19 pandemic. Sci. Adv. 6, eabd4998.